Cancer Imaging (2005) **5,** S57–S67
DOI: 10.1102/1470-7330.2005.0031

CI

e-med
www.e-med.org.uk

MULTIDISCIPLINARY SYMPOSIUM: HEAD & NECK CANCER

Monday 3 October 2005, 14:00–16:00

Lymph node imaging: multidetector CT (MDCT)

Paul M Silverman

Department of Radiology, University of Texas M. D. Anderson Cancer Center, Houston, TX, USA

Corresponding address: Paul M Silverman, MD, Department of Radiology, University of Texas M. D. Anderson Cancer Center, Houston, TX, USA
E-mail: psilverman@mdanderson.org

Abstract

Advances in cross-sectional imaging, including conventional and helical (spiral) CT and multidetector (MDCT) and MR imaging, now allow detailed evaluation of the anatomy and pathology of the neck and thoracic inlet. The major structures are identified by their appearance and that of contrasting fatty tissue planes surrounding the soft tissues. These structures include the larynx, trachea, thyroid, and parathyroid glands as well as the vessels, lymph node chains, nerves, and supporting muscles. A thorough understanding of the normal cross-sectional anatomy is fundamental to properly interpret pathologic processes. Pathologic processes include both solid and cystic masses. Most solid masses are enlarged lymph nodes. In contrast, cystic masses are of variable pathology, and their characteristic appearances and locations with respect to normal neck anatomy allow a confident diagnosis to be made from a brief differential diagnostic spectrum.

Keywords: *Neck; computed tomography (CT); lymph nodes.*

Technique

Computed tomography (CT) is performed with the patient supine in quiet respiration[1–4]. A pad placed beneath the patient's scapulae produces mild hyperextension of the neck and provides consistent images perpendicular to the long axis of the neck, minimizing dental artifacts. Scans are obtained using 3–5 mm or thinner contiguous slices. Multidetector CT (MDCT) affords optimal imaging in a single breath-hold, maximizing contrast enhancement and minimizing misregistration which improves visualization of small anatomic structures without rescanning or additional radiation. Intravenous contrast material is a prerequisite for enhancement of vascular structures. Its use facilitates differentiation of vessels from lymph nodes and the characterization of pathology.

Normal anatomy

The classic surgical approach divides the neck into two spaces, the anterior and posterior triangles (Fig. 1). The anterior triangle contains the major structures of the neck: hypopharynx, larynx, trachea, esophagus, thyroid, parathyroid, and salivary glands as well as the carotid sheath, nerves, and lymph nodes. Each anterior triangle is bordered posterolaterally by the sternocleidomastoid muscle and superiorly by the mandible. The anterior triangle is subdivided by the hyoid bone into suprahyoid and infrahyoid portions. The suprahyoid provides support for the floor of the mouth and contains sublingual, submandibular salivary glands and associated nodes. The infrahyoid portion contains the remaining components (Fig. 2). The posterior triangle is bounded anteriorly by the sternocleidomastoid muscle and posteriorly by the trapezius and is subdivided by the posterior belly of the omohyoid muscle. The space is primarily filled with fat and includes the hypoglossal nerve, vessels, and nodes.

Normal lymph nodes of the neck

The location of the various lymph node groups of the neck is most succinctly understood using a simplification of the Rouviere classification[5]. Nodal classification is

1470-7330/05/010057 + 11

Table 1 1997 AJCC nodal (N) staging systems for cervical lymph nodes

Level	Classification criteria
NX	The regional lymph nodes cannot be assessed (clinically)
N0	There are no regional metastatic lymph nodes present
N1	There is metastasis to a single ipsilateral lymph node that is 3 cm or less in greatest dimension
N2	There is metastasis in a single ipsilateral lymph node that is between 3 and 6 cm in greatest dimension; there are multiple ipsilateral lymph nodes, none of which are greater than 6 cm in greatest dimension; or there are bilateral or contralateral lymph nodes, none of which are greater than 6 cm in greatest dimension
N2a	There is metastasis in a single ipsilateral lymph node that is between 3 and 6 cm in greatest dimension
N2b	There are multiple ipsilateral lymph nodes, none of which are greater than 6 cm in greatest dimension
N2c	There are bilateral or contralateral lymph nodes, none of which are greater than 6 cm in greatest dimension
N3	There is metastasis in lymph nodes that are more than 6 cm in greatest dimension

critical for staging tumor extent[6–18]. Lymph nodes of the neck may be divided into 10 major groups[7–18].

The first six groups (I–VI) form a lymphoid collar at the junction of the head and neck (Fig. 2). These nodes are quite superficial, are usually accessible to palpation on physical examination and are commonly referred to as collar nodes: occipital, mastoid, parotid, submandibular, and facial submental.

Two groups of nodes lie deep within this lymphoid collar and are not accessible to clinical examination. Pathologic enlargement (>1.5 cm) allows detection. These nodes—groups VII, sublingual, and VIII, retropharyngeal—are often the site of metastases from carcinoma of the nasopharynx, the base of the tongue, and the tonsils (Fig. 3).

The anterior cervical group (IX) consists of superficial (Fig. 4B) and deep components (Fig. 4C). These nodes may be the site of metastases from primary tumors in the thyroid, larynx, and lung.

The lateral cervical nodes (group X) are also composed of superficial and deep chains (Fig. 5). This important deep group of nodes consists of three chains that form a triangle. The anterior portion is the internal jugular chain, the posterior portion is the spinal accessory chain, and the inferior component is the transverse cervical chain. Of these groups, the most important in staging head and neck tumors are the nodes along the internal jugular chain. A classification used by our surgical colleagues is shown in Table 1. Although the table is useful, the classification can easily be integrated into our system by carefully describing in reports the anatomic location of the nodes.

A new imaging-based classification for abnormal nodes

Recently, the results of a study produced an imaging-based nodal classification for the evaluation of metastatic neck adenopathy. Imaging landmarks were identified to create a nodal classification similar to that of the American Joint Committee on Cancer and the American Academy of Otolaryngology—Head and Neck Surgery[9–11,18–24] (Table 2). This system was defined to ensure a more consistent nodal classification and to eliminate confusion with existing clinically based classifications. Imaging was chosen as a pivotal study because it identifies clinically silent nodes. Table 2 summarizes this new imaging-based classification (Figs. 6–19). A roman numeral is used to define the levels referenced to anatomic names, such as supraclavicular, retropharyngeal, carotid, facial, occipital, postauricular, and other superficial nodes; these anatomic terms are still widely used. This classification brings some improved precision and reproducibility to the staging of head and neck diseases.

Nodal disease

Clinical examination alone is highly inaccurate in staging nodal disease in patients with head and neck tumors. Therefore, prophylactic X-ray therapy can be used to treat patients with occult metastases, which are estimated to occur in 15%–20% of these individuals.

Because normal nodes in the neck may be identified on high-quality scans, criteria have been established to define lymphadenopathy: (1) a discrete mass great than 1.0–1.5 cm; (2) an ill-defined mass in a lymph node area; (3) multiple nodes of 6–15 mm; and (4) obliteration of tissue planes around vessels in a nonirradiated neck. A nodal mass with central low density is specifically indicative of tumor necrosis[5–8].

Less common, nonnodal solid masses include neurovascular tumors (paraganglioma, neurofibroma, hemangioma), primary neoplasms (fibroma, sarcoma), congenital lesions (teratoma, ectopic thyroid), trauma (hematoma), lesions of the bone (plasmacytoma, aneurysmal bone cyst), and infection. Specific imaging features aid the differential diagnosis. Paragangliomas

(1)

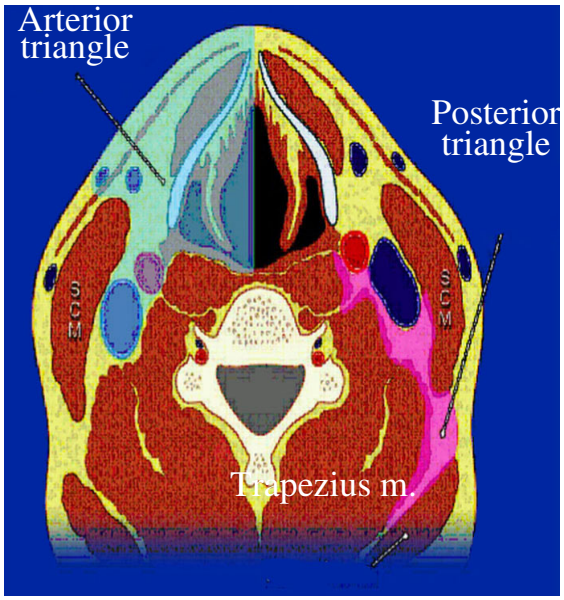

(2A)

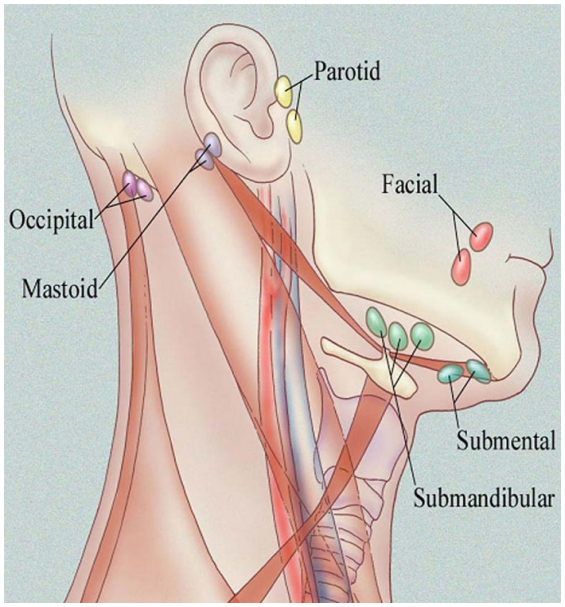

(2B)

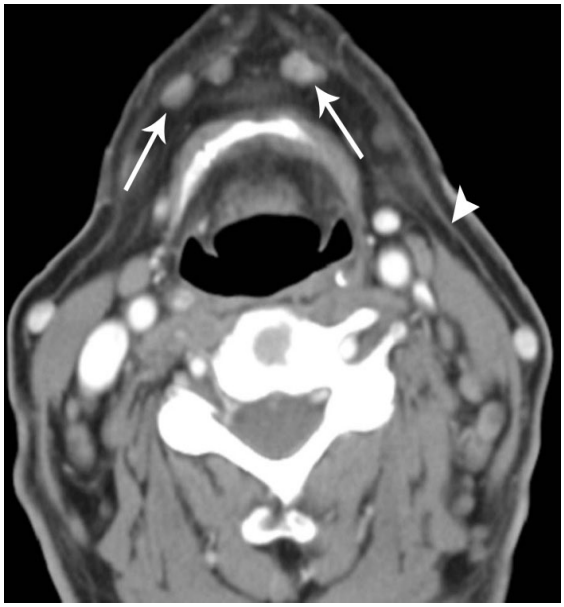

(2C)

Figures 1–2. **(1) Cross-sectional diagram. Anterior and posterior triangle of the neck. (2) (A) Collar nodes. There are six (I–VI) major nodal groups at the junction of the head and neck. The posterior group consists of the carotid, occipital, and mastoid group while the anterior group consists of the facial, submental, and submandibular nodes. They form a collar of rather superficial nodes. (B) CT scan at the level of the hyoid. Multiple non-specific submental nodes (arrow) deep to the platysmal muscle (arrowhead). (C) Scattered submandibular sub-centimeter nonspecific nodes seen lateral to the submandibular glands (arrows).**

Table 2 Clinical classification of neck nodes

t	Definition of nodes
I	Above hyoid bone Below mylohyoid muscle Anterior to back of submandibular gland
IA	Between medial margins of anterior bellies of digastric muscles Previously classified as submental nodes
IB	Posterolateral to level IA nodes Previously classified as submandibular nodes
II	From Skull base to level of lower body of hyoid bone Posterior to back of submandibular gland Anterior to back of sternocleidomastoid muscle
IIA	Anterior, lateral, medial, or posterior to internal jugular vein Inseparable from internal jugular vein (if posterior to vein) Previously classified as upper internal jugular nodes
IIB	Posterior to internal jugular vein with pat plane separating nodes and vein Previously classified as upper spinal accessory nodes
III	From level of lower body of hyoid bone to level of lower cricoid cartilage arch Anterior to back of sternocleidomastoid muscle Previously known as mid jugular nodes
IV	From level of lower cricoid cartilage arch to level of clavicle Anterior to line connecting back of sternocleidomastoid muscle and posterolateral margin of anterior scalene muscle Lateral to carotid arteries Previously known as low jugular nodes
V	Posterior to back of sternocleidomastoid muscle from skull base to level of lower cricoid arch From level of lower cricoid arch to level of clavicle as seen on each axial scan Posterior to line connecting back of sternocleidomastoid muscle and posterolateral margin of anterior scalene muscle Anterior to anterior edge of trapezius muscle
VA	From skull base to level of bottom of cricoid cartilage arch Posterior to back of sternocleidomastoid muscle Previously known as upper level V nodes
VB	From level of lower cricoid arch to level of clavicle as seen on each axial scan Posterior to line connecting back of sternocleidomastoid muscle and posterolateral margin of anterior scalene muscle Previously known as lower level V nodes
VI	Between carotid arteries from level of lower body of hyoid bone to level superior to top of manubrium Previously known as visceral nodes
VII	Between carotid arteries below level of top of manubrium Caudal to level of innominate vein Previously known as superior mediastinal nodes
Supraclavicular	At or caudal to level of clavicle as seen on each axial scan Above and medial to ribs
Retropharyngeal	Within 2 cm of skull base and medial to internal carotid arteries

(carotid body tumor) occur in the carotid space and consistently show early and persistently dense enhancement after the administration of contrast material. Acute hematomas are characterized by an intrinsically high CT attenuation and high intensity on T1-weighted magnetic resonance (MR) imaging. Metastases are located in the expected site of the major lymph node chains of the neck. Many investigators now use 1.0 cm as an effective size criteria for positive nodes in a patient population at high risk. Nodes in the upper neck tend to be large because of repeated respiratory infections; therefore, more liberal size criteria should be accepted. With the use of more liberal criteria, 80% of nodes will be metastatic and 20% will be benign hyperplastic. Important caveats include the follow: (1) regardless of primary site, a single ipsilateral node decreases survival by 50% and a contralateral node halves survival again; (2) extranodal extension is the best indicator of treatment failure and decreases survival by 50%; (3) posterior triangle nodes, with the exception of lymphoma, indicate a poor prognosis; and (4) nodes in the low internal jugular chain have a poor prognosis because proximal spread has often occurred. These caveats are helpful when dealing with the assessment of lymphadenopathy in this region.

(3A)

(3B)

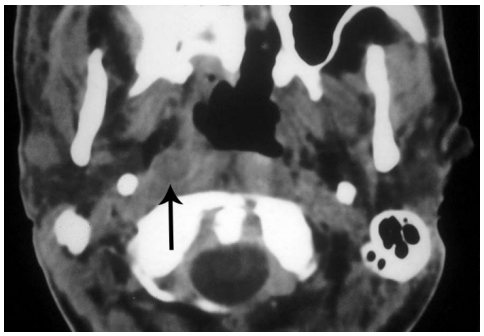

(4A)

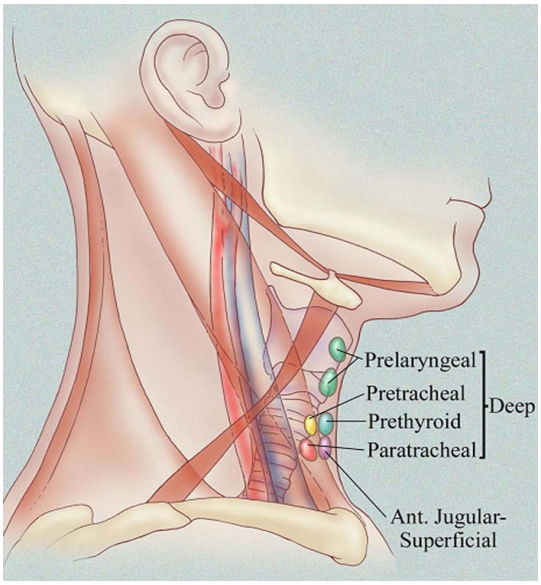

(4B)

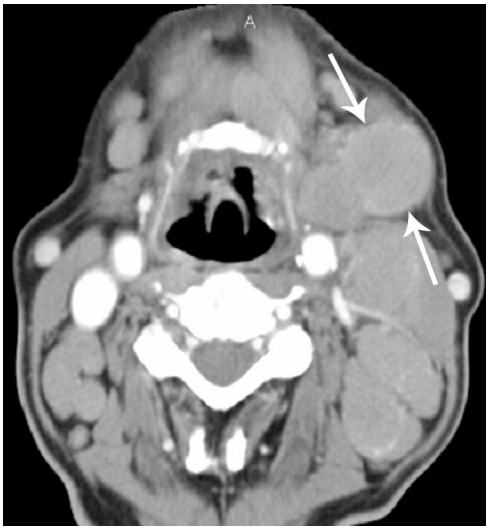

(4C)

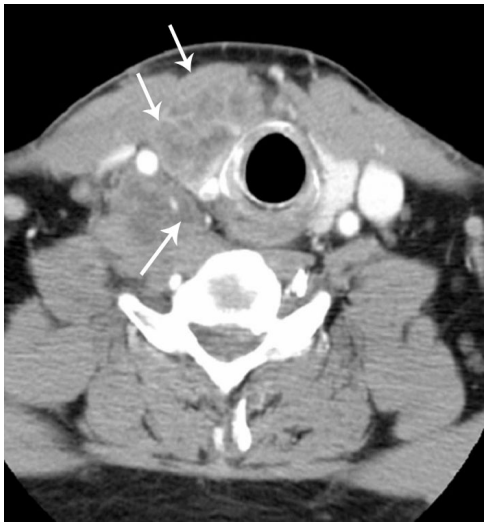

Figures 3–4. **(3) (A) Groups VII and VIII are the sublingual and retropharyngeal nodes. The sublingual nodes are not specifically accessible by cross-sectional imaging but the retropharyngeal nodes are blind to clinical assessment and dependent on radiologic imaging. Diagram at the level of the posterior pharynx demonstrates retropharyngeal nodes in light blue. (B) CT scan showing low attenuation, necrotic node in the right retropharyngeal region (arrow). (4) (A) Anterior cervical nodes (IX). This consists of superficial and deep components. The superficial group is along the anterior jugular vein and the deep group consists of the pre-laryngeal, pre-tracheal, pre-thyroid, and paratracheal nodes. (B) CT scan showing lymphadenopathy including the anterior jugular region (arrow) in a patient with lymphoma. (C) CT scan demonstrating numerous deep nodes along the thyroid gland from metastatic disease.**

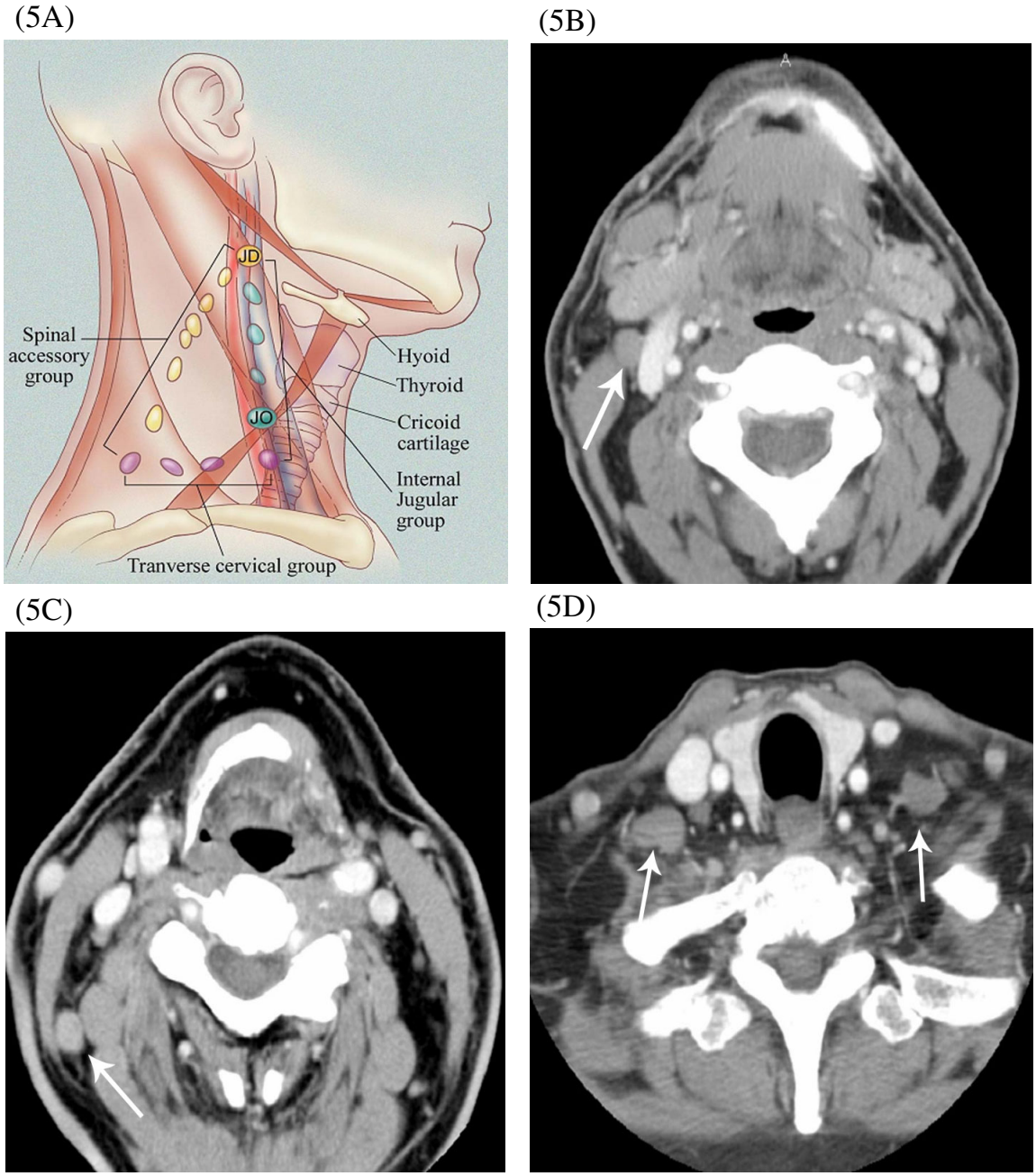

Figure 5. **(A) Lateral cervical nodes (X). The lateral cervical nodes are composed of three chains: the spinal accessory chain in the posterior triangle of the neck, the internal jugular chain along the internal jugular vein, and transverse cervical chain along the base of this triangle. The internal jugular chain represents the major site of metastatic disease for head and neck primary tumors. JD, jugulodigastric node; JO, juguloomohyoid node. (B) CT scan showing node (arrow) seen just lateral to the right internal jugular vein within the right internal jugular group. (C) Small node seen in the distribution of the spinal accessory group (arrow). (D) Enlarged nodes in the transverse cervical chain at the base of the neck (arrows).**

(6)

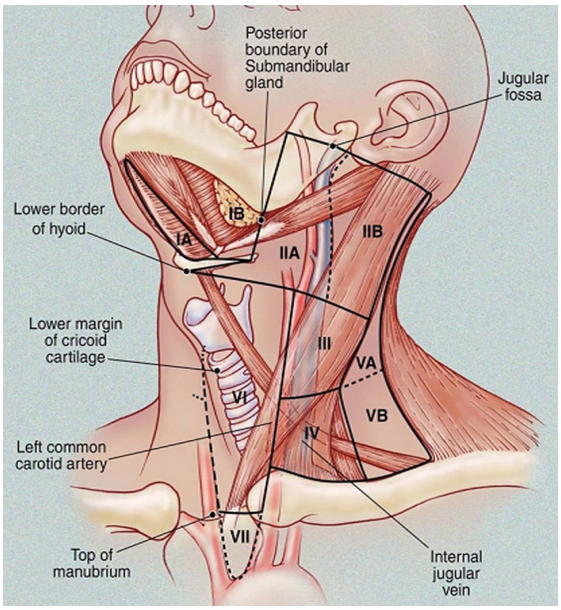

(7)

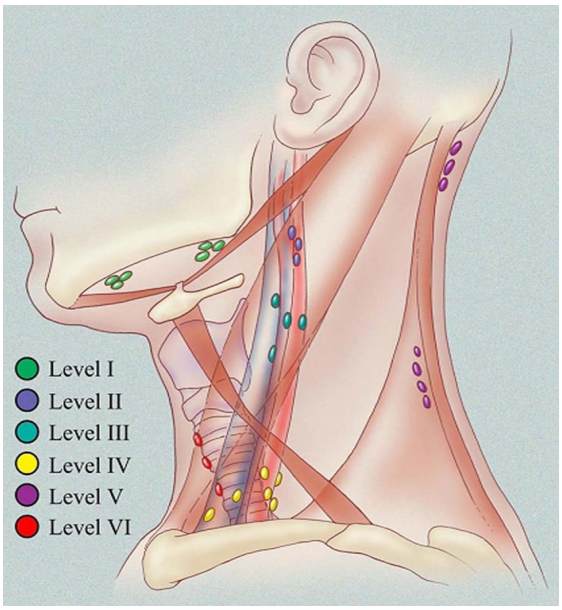

(8)

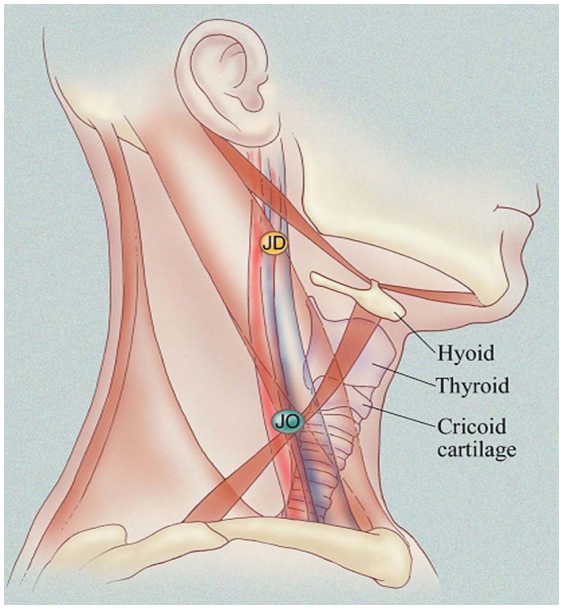

Figures 6–8. **(6) Imaging-based classification of neck nodes as defined in Table 1. These nodes are labeled I–VII with an additional notation of supraclavicular and retropharyngeal nodes. Adapted from: Som and Brandwein[24]. (7) Diagrammatic representation showing the distribution of nodes and their levels. Adapted from: Som and Brandwein[24]. (8) Internal jugular chain nodes. Diagrammatic demonstration of the superior and inferior extents of the internal jugular chain. The largest node superiorly in the internal jugular chain is the jugulodigastric node just posterior to the posterior belly of the digastric muscle. The largest inferior node is the jugulo-omohyoid node which lies along the intersection of the sternocleidomastoid muscle and the omohyoid muscle. Adapted from: Som and Brandwein[24].**

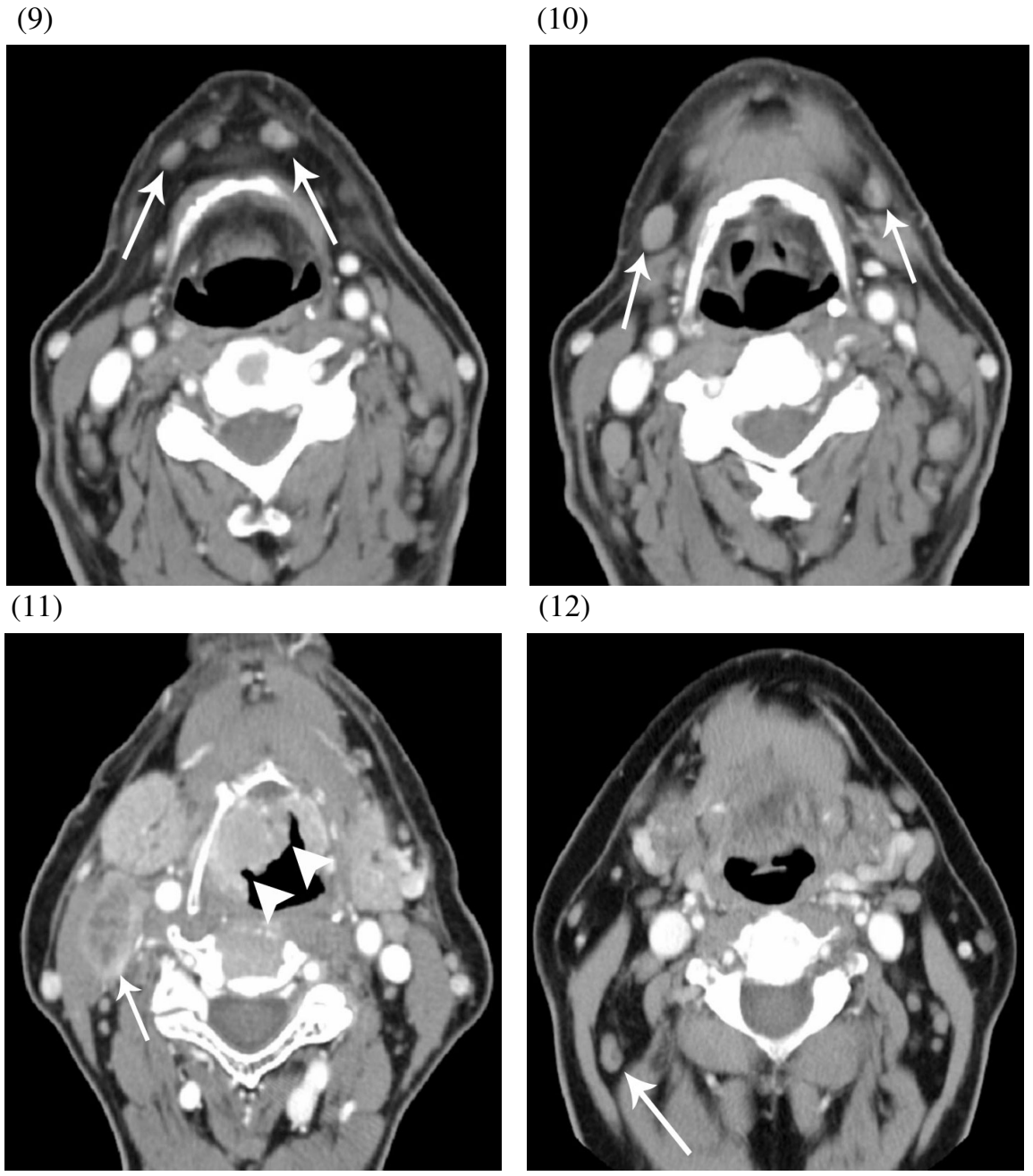

Figures 9–12. **(9) Level IA, submental nodes. CT scan at the level of the hyoid bone showing multiple nodes superficially (arrows). (10) Level IB, submandibular nodes. CT scan at the level of the body of the hyoid demonstrates nodes just lateral to the hyoid bone (arrow). (11) Level IIA, upper internal jugular chain. CT scan at the level of the hyoid bone. Necrotic node in the area of the high internal jugular chain (arrow). Necrotic node is the result of metastasis from pyriform sinus cancer (arrowheads). (12) Level IIB, upper spinal accessory chain. CT scan at the level of the upper neck demonstrating nodes (arrow) which were previously classified as upper spinal accessory nodes in the posterior triangle.**

(13)

(14)

(15)

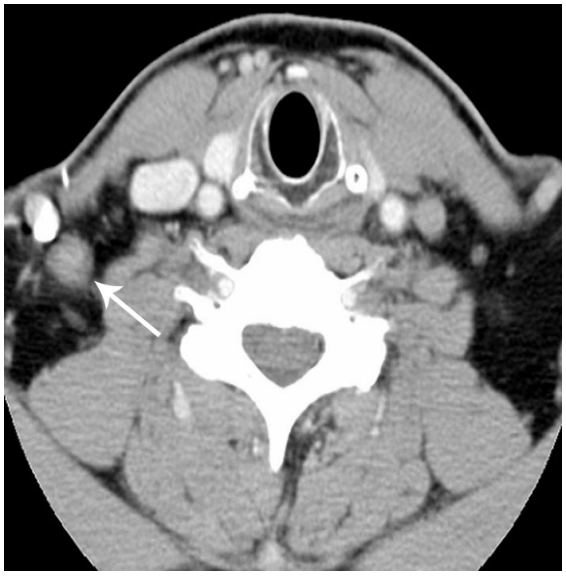

(16)

Figures 13–16. **(13) Level III. Nodes previously described as mid-internal jugular chain nodes. CT scan at the level of the mid-internal jugular (arrows). (14) Level IV. Low internal jugular chain. CT scan demonstrating adenopathy in the low internal jugular chain (arrows). (15) Level V. Low spinal accessory chain. CT scan demonstrating node in the low posterior triangle region on right (arrow). (16) Level VI. Nodes previously described as juxtavisceral nodes. CT scan demonstrating small nodes (arrow) along the area of the thyroid gland.**

(17)

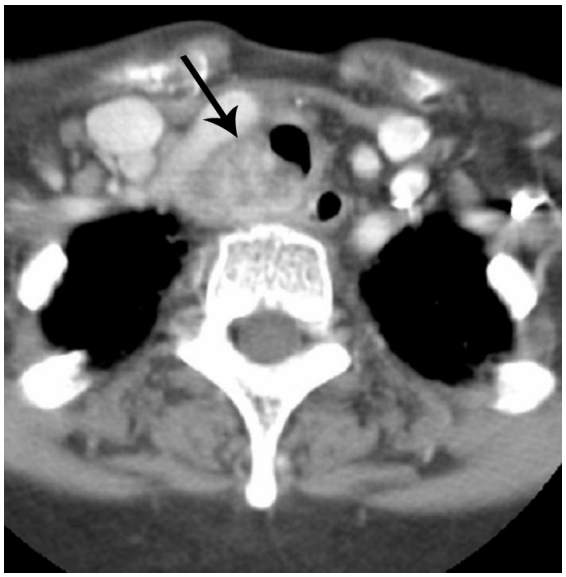

(18)

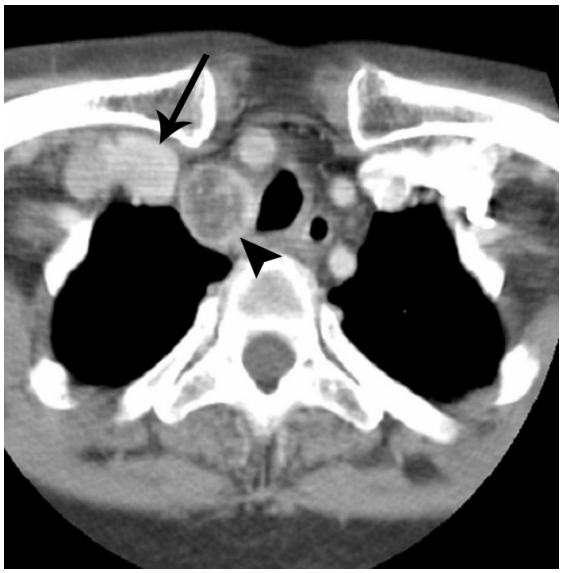

(19)

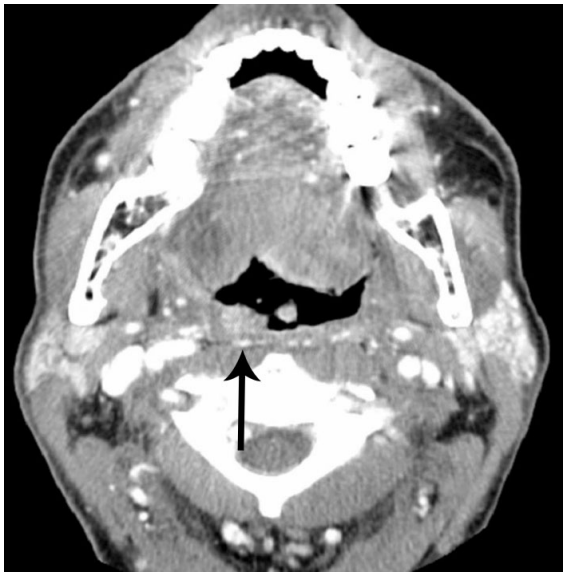

Figures 17–19. **(17) Level VII. Superior mediastinal nodes. CT scan demonstrating nodes in the superior mediastinum from head and neck primary (arrow). (18) Supraclavicular nodes. CT scan at the level of the medial aspect of the clavicles demonstrates an enlarged node in the right paratracheal region (arrowhead) and right supraclavicular node (arrow). (19) Retropharyngeal nodes. CT scan at the level of the base of the tongue demonstrates a small enhancing node in the right retropharyngeal area (arrow), a region blinded to clinical examination because of its location deep to the mucosa.**

In summary, careful analysis of nodes in the neck and knowledge of the various compartments is critical in the assessment and staging of primary head and neck malignancies.

References

[1] Reede DL, Whelan MA, Bergeron RT. Computed tomography of the infrahyoid neck, parts I and II. Radiology 1982; 145: 389–402.

[2] Mancuso AA, Maceri D, Rice D, Hanagee W. CT of cervical lymph node cancer. AJR 1981; 135: 381–5.

[3] Silverman PM, Korobkin M, Moor AV. Computed tomography of cystic neck masses. J Comput Assist Tomogr 1983; 7: 498–502.

[4] Mancuso AA, Hanafee W. Computed Tomography and Magnetic Resonance Imaging of the Head and Neck, 2nd edn. Baltimore, MD: Williams & Wilkins, 1985.

[5] Rouviere H. Lymphatic System of the Head and Neck, Ann Arbor, MI: Edwards, 1983.

[6] Svojanen JN, MvKherji SK, Supuy DE, Takahashi JH, Costello P. Spiral CT in evaluation of head and neck lesions. Radiology 1992; 183: 281–3.

[7] Van den Brekel MWM, Castelings JA, Snow G. Detection of lymph node metastases in the neck: radiologic criteria. Radiology 1994; 192: 617–8.

[8] Som PM. Detection of metastasis in cervical lymph node: CT and MR criteria and differential diagnosis. AJR 1992; 158: 961–9.

[9] Spiro RH. The management of neck nodes in head and neck cancer: a surgeon's view. Bull NY Acad Med 1985; 61: 629–37.

[10] Beahrs OH, Henson DE, Hutter RVP *et al*. Manual for Staging Cancer, 3rd edn. Philadelphia, PA: Lippincott, 1988.

[11] Robbins KT. Pocket Guide to Neck Dissection and TNM Staging of Head and Neck Cancer, Alexandria, VA: American Academy of Otolaryngology—Head and Neck Surgery Foundation, 1991: 1–31.

[12] Lindberg R. Distribution of cervical lymph node metastases from squamous cell carcinoma of the upper respiratory and digestive tracts. Cancer 1972; 29: 1446–9.

[13] Van den Brekel MWM. Assessment of Lymph Node Metastases in the Neck: A Radiological and Histopathological Study, Utrecht: University of Amsterdam, 1992: 1–152.

[14] Fleming ID, Cooper JS, Henson DE *et al*. American Joint Committee on Cancer Staging Manual, 5th edn. Philadelphia, PA: Lippincott–Raven, 1997.

[15] Feinmesse R, Freeman JL, Nojek AM *et al*. Metastatic neck disease: a clinical/radiographic/pathologic correlative study. Arch Otolaryngol Head Neck Surg 1987; 113: 1307–10.

[16] Close LG, Merkel M, Vuitch MF *et al*. Computed tomographic evaluation of regional lymph node involvement in cancer of the oral cavity and oropharynx. Head Neck 1989; 11: 309–17.

[17] Stevens MH, Harnsberger R, Mancuso AA *et al*. Computed tomography of cervical lymph nodes: staging and management of head and neck cancer. Arch Otolaryngol Head Neck Surg 1985; 111: 735–9.

[18] Som PM, Curtin HD, Mancuso AA. An imaging-based classification for the cervical nodes designed as an adjunct to recent clinically based nodal classifications. Arch Otolaryngol Head Neck Surg 1999; 125: 388–96.

[19] Som PM, Curtin HD, Mancuso AA. Imaging-based nodal classification for evaluation of neck metastatic adenopathy. AJR 2000; 174: 837–44.

[20] Mancuso AA, Hamsberger HR, Muraki AS, Stevens MH. Computed tomography of cervical and retropharyngeal lymph nodes: normal anatomy, variants of normal, and applications in staging head and neck carcinoma, parts I and II. Radiology 1983; 148: 709–23.

[21] Robbins KT, Medina JE, Wolfe GT *et al*. Standardizing neck dissection terminology. Arch Otolaryngol Head Neck Surg 1991; 117: 601–5.

[22] Lindberg RD. Distribution of cervical lymph node metastases from squamous cell carcinoma of the upper respiratory and digestive tracts. Cancer 1972; 29: 1448–9.

[23] Husband JES, Reznek RH. Imaging in Oncology: Tumors of the Pharynx, Tongue, and Mouth, 2nd edn. Oxford: ICIS Medical Media Ltd, 2004.

[24] Som PM, Brandwein MS. Lymph Nodes in Head and Neck Imaging, 4th edn. St. Louis, MO: Mosby, 2003.